



NP06/ENUBET annual report 2022 for the SPSC

The ENUBET Collaboration

F. Acerbi^{a,b}, I. Angelis^x, L. Bomben^{e,p}, M. Bonesini^e, A. Branca^{e,f}, F. Bramati^{e,f},
 C. Brizzolari^{e,f}, G. Brunetti^f, M. Calviani^r, S. Capelli^{e,p}, S. Carturan^{d,g}, M.G. Catanesi^h,
 S. Cecchiniⁱ, N. Charitonidis^r, F. Cindoloⁱ, G. Cogo^d, G. Collazuol^{c,d}, F. Dal Corso^c,
 C. Delogu^{c,d}, G. De Rosa^{j,k}, A. Falcone^{e,f}, B. Goddard^r, A. Gola^a, F. Iacob^{c,d}, C. Jollet^l,
 V. Kain^r, B. Kliček^m, Y. Kudenko^{n,u,v}, Ch. Lampoudis^x, M. Laveder^{c,d}, A. Longhin^{c,d},
 L. Ludovici^o, E. Lutsenko^{e,p}, L. Magaletti^{h,q}, G. Mandrioliⁱ, A. Margottiⁱ, V. Mascagna^{y,z},
 N. Mauriⁱ, L. Meazza^{e,f}, A. Meregaglia^l, M. Mezzetto^c, M. Nessi^r, A. Paoloni^t, M. Pari^{c,d,r},
 E.G. Parozzi^{e,f,r}, L. Pasqualini^{i,s}, G. Paternoster^a, L. Patriziiⁱ, M. Pozzatoⁱ, M. Preste^{e,p},
 F. Pupilli^{c,d}, E. Radicioni^h, A.C. Ruggeri^{j,k}, D. Sampsonidis^x, C. Scian^{c,d}, G. Sirriⁱ,
 M. Stipčević^m, M. Tentiⁱ, F. Terranova^{e,f}, M. Torti^{e,f,l}, S. E. Tzamarias^x, E. Vallazza^e,
 F.M. Velotti^r, and L. Votano^t

^aFondazione Bruno Kessler (FBK), Via Sommarive 18 - 38123 Povo (TN), IT

^bINFN-TIFPA, Università di Trento, Via Sommarive 14 - 38123 Povo (TN), IT

^cINFN Sezione di Padova, via Marzolo 8 - 35131 Padova, IT

^dUniversità di Padova, via Marzolo 8 - 35131 Padova, IT

^eINFN Sezione di Milano-Bicocca, Piazza della Scienza 3 - 20133 Milano, IT

^fUniversità di Milano-Bicocca, Piazza della Scienza 3 - 20133 Milano, IT

^gINFN, Laboratori Nazionali di Legnaro, Viale dell'Università 2 - 35020 Legnaro (PD), IT

^hINFN Sezione di Bari, Via Giovanni Amendola 173 - 70126 Bari, IT

ⁱINFN Sezione di Bologna, viale Berti-Pichat 6/2 - 40127 Bologna, IT

^jINFN, Sezione di Napoli, Strada Comunale Cinthia - 80126 Napoli, IT

^kUniversità "Federico II" di Napoli, Corso Umberto I 40 - 80138 Napoli, IT

^lCENBG, Université de Bordeaux, CNRS/IN2P3, 33175 Gradignan, FR

^mCenter of Excellence for Advanced Materials and Sensing Devices, Ruder Boskovic Institute, HR-10000 Zagreb, HR

ⁿ Institute for Nuclear Research of the Russian Academy of Sciences, 117312 Moscow, RU

^oINFN Sezione di Roma 1, Piazzale A. Moro 2, 00185 Rome, IT

^pUniversità degli Studi dell'Insubria, Via Valleggio 11 - 22100 Como, IT



^qUniversità degli Studi di Bari, Via Giovanni Amendola 173 - 70126 Bari, IT

^rCERN, Esplanade des particules - 1211 Genève 23, CH

^sUniversità degli Studi di Bologna, viale Berti-Pichat 6/2 - 40127 Bologna, IT

^tINFN, Laboratori Nazionali di Frascati, via Fermi 40 - 00044 Frascati (Rome), Italy

^uNational Research Nuclear University “MEPhI”, 115409 Moscow, Russia

^vMoscow Institute of Physics and Technology, 141701 Moscow region, Russia

^xAristotle University of Thessaloniki. Thessaloniki 541 24, Greece.

^yDII, Università degli Studi di Brescia, via Branze 38, Brescia, Italy.

^zINFN, Sezione di Pavia, via Bassi 6, Pavia, Italy.

31 March 2022

Contents

1	Executive summary	2
1.1	Demonstrator construction	3
1.1.1	Status of procurement and construction	5
1.1.2	Test beam of November 2021	7
1.2	Design of the hadronic beamline	7
1.3	Assessment of systematic uncertainties	11
1.4	Collaboration, synergies with other projects	15

1 Executive summary

The last year has been a very intense and fruitful period for ENUBET with several significant advances along the following directions:

1. the detector R&D with a prominent effort being dedicated to the finalization of the ENUBET demonstrator (Sec. 1.1).
2. the design of the hadronic beamline has undergone a significant step forward in quality with the implementation of very interesting and ambitious optimization algorithms (Sec. 1.2).
3. the assessment of systematics on the neutrino flux has been cast into a consistent framework that has allowed to test, for the first time, the reduction of the uncertainty on the flux related to hadroproduction after fitting the distributions of measured leptons (positive muons and positrons) (Sec. 1.3).

4. we have started exploring the possibility of possible synergies with the nuSTORM project with a dedicated session in the context of the NuFact workshop that was held in Cagliari (IT) in September 2021 (Sec. 1.4).

We will in the following concentrate on the advances with respect to the previous report where we gave a more comprehensive overview[1] of the project.

1.1 Demonstrator construction

The layout of the demonstrator is shown in Fig. 1. The goal is to prove the performance, cost-effectiveness and scalability of tagger detector concept i.e. a sampling calorimeter (e^+ , π^+ , μ^+ PID and energy measurement) with a light tracker (t_0 -layer) in the innermost region (for e/π^0 separation). The demonstrator is 1.65 m long in the longitudinal direction and it spans 90° in azimuth. The inner radius is 1 m.

The central 45° central region will be instrumented and readout while the rest will prove the mechanical requirements. The structure is designed to be extendable to a full 2π object by joining four similar detectors with minimal dead regions.

The demonstrator comprises 75 layers of iron (15 mm thick) and 75 layers of scintillators (7 mm thick). The instrumented fraction (50%) corresponds to $15(z) \times 3(r) \times 25(\phi)$ ¹ (=1125) calorimeter channels and $15(z) \times 2(\text{layers}) \times 25(\phi)$ (=750) t_0 -layer channels, with 1875 channels in total.

The iron part extends radially for 11 cm while the remaining 30 cm are filled with 22 mm thick with Borated P.E. slabs with 5% Boron (BPE, green in the figures). A section of the detector corresponding to the basic unit in z , is shown in Fig. 2, left.

The overall detector is held by a mechanical crawl sitting on four extensible legs that are designed to allow tilting the calorimeter-beam angle in the vertical plane and adjusting the horizontal position by means of a wheel-rail mechanism. The total weight is 7 ton.

The layout of scintillators is shown in Fig. 2, left. All tiles are trapezoidal in shape such that to minimize dead regions, with transverse dimensions of $\sim 3 \times 3$ cm². The t_0 -layer tile (innermost radial position) holds two grooves. They are 1 mm deep such that the full WLS diameter is enclosed in the scintillator. These two grooves are meant for light collection (“readout” grooves) and they are propagated to the other three outer tiles where they only have the function of letting space to host the WLS fiber without letting the scintillation light to enter (“transit” grooves). Transit grooves hence need to be covered with a chemical etching treatment to make them optically opaque. The second tile has readout grooves on the other side of the transit grooves. This pattern repeats as in the Figure. For tile 2 and 3 readout grooves are slightly offset-ed with respect to 0 and 1 to accommodate them with the transit ones.

¹We denote with z the coordinate along the cylinder axis and with r and ϕ the radial and azimuthal coordinates respectively.



Figure 1: Left: 3D rendering of the demonstrator. Right: assembly at INFN-LNL.

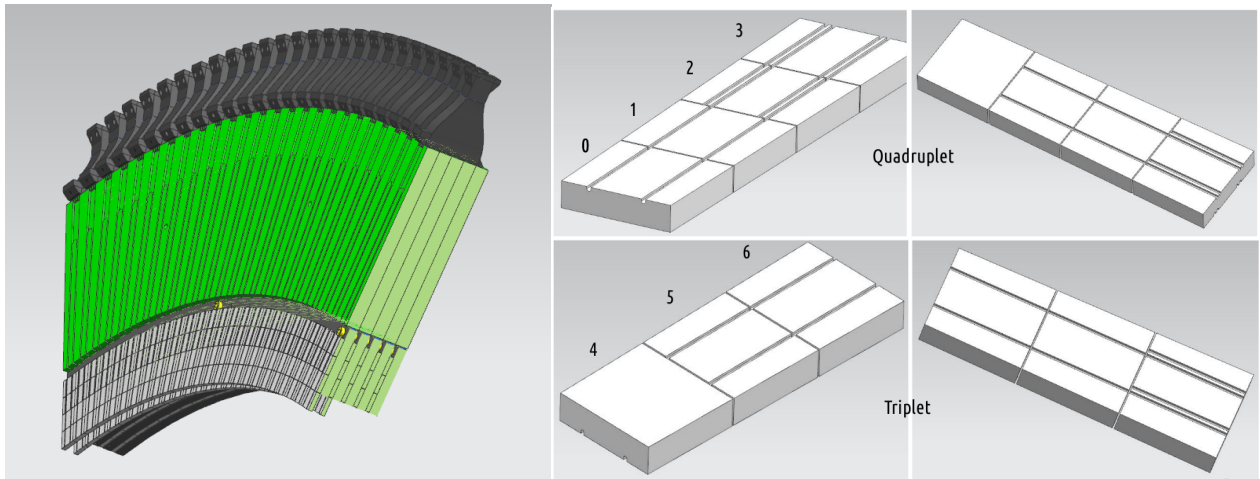


Figure 2: Left: rendering of a section of the demonstrator corresponding to the extension along the beam axis of single module (LCM). Scintillators are shown in gray, borated polyethylene shielding in green and fiber concentrators in black. Right: layout of the frontal grooves readout scheme.

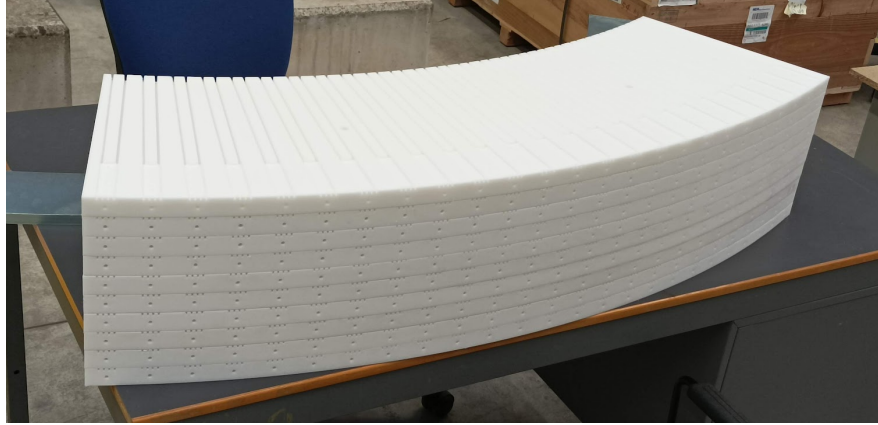


Figure 3: The borated polyethylene shielding slabs.

Ten WLS fibers belonging to the same LCM are routed by passing through grooves milled in the BPE slabs (Fig. 3) and bundled to a $4 \times 4 \text{ mm}^2$ SiPM. The t_0 -layer fibers will be read by two independent $3 \times 3 \text{ mm}^2$ SiPMs .

The demonstrator will adopt WLS fiber “concentrators” that we developed using 3D-printing techniques. These objects (Fig. 4) are essential to ease the process of fibers bundling. In such a way the coupling of WLS fibers to the SiPM can be accomplished in a neat and reproducible way allowing a good, homogeneous optical contact. After fiber polishing, five SiPM (three $4 \times 4 \text{ mm}^2$ and two $3 \times 3 \text{ mm}^2$ for the t_0 -layer), soldered on a $7 \times 4 \text{ cm}^2$ PCB (Front-end, FE board), will be fixed to the top of each fiber concentrator with screws.

1.1.1 Status of procurement and construction

The tests of the demonstrator at CERN are scheduled for October 2022 (weeks 40 and 41) at the CERN-PS/T9 beamline.

- **Structure.** The mechanical structure is basically finalized as it can be seen in Fig. 1, right. It shows the current status of the prototype at INFN-LNL where it is being assembled. The telescopic legs have also been delivered and the only remaining step is mounting the base and the system of rails for the horizontal displacement, shown in black and beige in Fig. 1, left. The 75 iron arcs and 150 BPE arcs are also ready for assembly (partially visible in Fig. 1, right). The darkening of the setup will be achieved with an extendable box made with plastic and the additional covering with a thick black tissue (in delivery).
- **WLS fibers.** The WLS fibers Y-11 double clad 1 mm diameter have also been delivered from Kuraray (JP).
- **Fiber concentrators.** We have printed about 25% of the total needed (375) with a battery of five commercial 3D printers. The total production can be finalized within ~ 1 month with

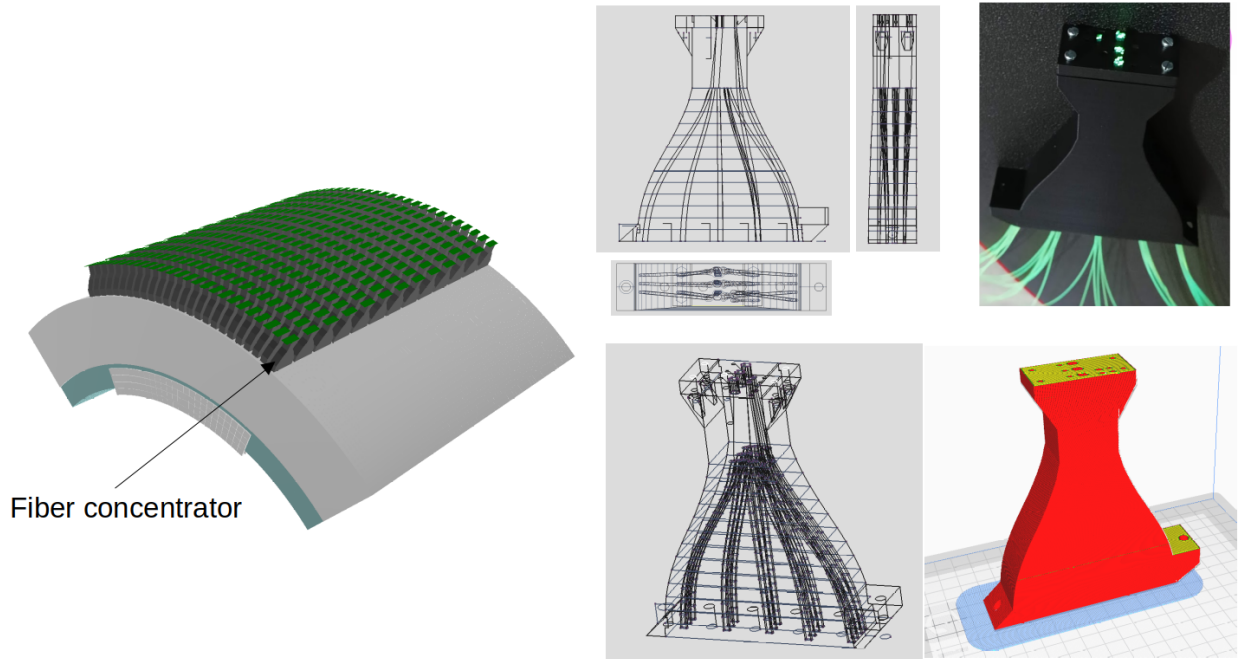


Figure 4: Fiber concentrators.

limited manpower.

- **Photo-sensors.** The procurement of Silicon Photomultipliers for the ENUBET demonstrator has been finalized and Hamamatsu models S14160-3050HS ($3 \times 3 \text{ mm}^2$) and S14160-4050HS ($4 \times 4 \text{ mm}^2$) were selected.
- **Electronics.** A prototype digital board to handle the signals from a 4 channel ADC board (250 MS/s, 14 bit) and to provide a USB interface with the PC has been designed around an Altera 5CGXBC3B6F23I7N FPGA and manufactured. It is undergoing extensive tests in order to validate the different parts. These boards are unfortunately not mature enough for a large scale production but their performances will nevertheless be tested on a more limited amount of channels. To compensate for this reduction, in the readout of the final ENUBET prototype this custom electronics will be complemented and cross-checked with about 20 commercial digitizers that are partially available in the labs and partially will be hired at the CERN electronics pool. In addition a set of twenty 64-ch boards by CAEN (A5202) based on the WeeROC CitiROC-1A ASICs will be employed. In this case they will only readout the signals' amplitudes and times for a total of 1280 channels. These boards are being delivered by the company. The remaining channels will be read-out using 96-ch boards (also based on the CitiROC ASIC) previously developed by the Baby-MIND collaboration. The development of a common DAQ is in progress. The front-end boards that will be mounted on the concentrators have been designed and pre-produced (in 32 pieces). The signals will be sent to the readout

boards with very thin coaxial cables by HIROSE. We are finalizing the procurement of the components and the design of the interface boards to match the output of the FE boards and A5202 cards.

- **Scintillators.** The most critical part is currently the production and machining of the scintillators tiles. The scintillators are in the production phase with UNIPLAST (Moscow) in collaboration with the INR group. The press form for the plastic injection molding has been finalized and a first set of some hundreds tiles produced and tested for light yield with very good results. The total number of needed tiles is 6375, in seven different shapes. The delivery of materials and transactions are evidently critical due to the international situation. In view of the high probability of delays we have made contacts with a company that could likely perform the production with milling techniques instead of using injection molding, starting on scintillator sheets that are being procured by SCIONIX. The first scintillator tiles specimen with this alternative plan are awaited these days. The prospect is promising and will imply some additional waste of material which is intrinsic in the milling procedure due to the size of the milling drive of a few mm.

1.1.2 Test beam of November 2021

A pre-demonstrator small prototype comprising 3 LCMs (ENUBINO) (Fig. 5) has been built and characterized with cosmic ray tracks at INFN-LNL laboratory and with particle beams at CERN in November 2021 (Fig. 6). It faithfully implements the chosen geometry and the solutions for the light readout both at the level of scintillators and of the neutron absorber layer. The prototype behaves according to expectations with a good uniformity and a tolerable level of optical cross talk between the scintillator tiles. Efficiency maps show high efficiency and good uniformity (Fig. 7, left). The response to m.i.p signals was also tested with the final selected Hamamatsu SiPM model as a function of the supply voltage (Fig. 7, right). The cross-talk between the signals is also being characterized and the results will be made public soon.

1.2 Design of the hadronic beamline

The optimization of the beamline ([2]) is one of the pillars of the project and it implies a careful analysis of a multi-parametric problem (choice of fields, collimators, apertures) in order to produce an intense and well collimated beam of kaons and pions in the tagger volume. Since the beginning our guideline has been that of employing standard magnets with moderate apertures. Traditionally the optics optimization has been performed using TRANSPORT and then the system has been ported to G4beamline to simulate re-interactions of stray particles and background in the tagger. With time we have developed a very powerful simulation in GEANT4 with the possibility of controlling via external control cards all the parameters of the system. This has opened the way to a more systematic optimization of the beamline leveraging on the work done for optimizing the shape of the horn [1] which led to the development of a rather general optimization framework based on a genetic algorithm. This algorithm has been applied to a first systematic scan acting on 5

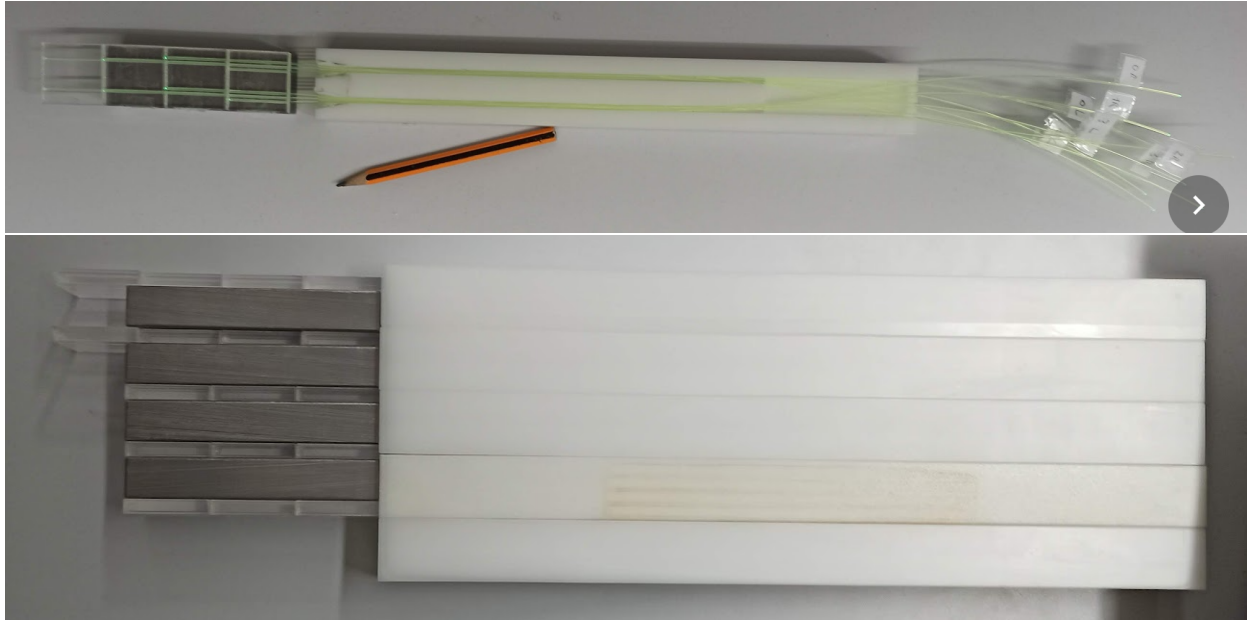


Figure 5: Prototype of a single azimuthal section of the demonstrator (ENUBINO) shown during its assembly to highlight the composing elements (scintillators, iron absorbers, WLS fibers and the BPE shielding).

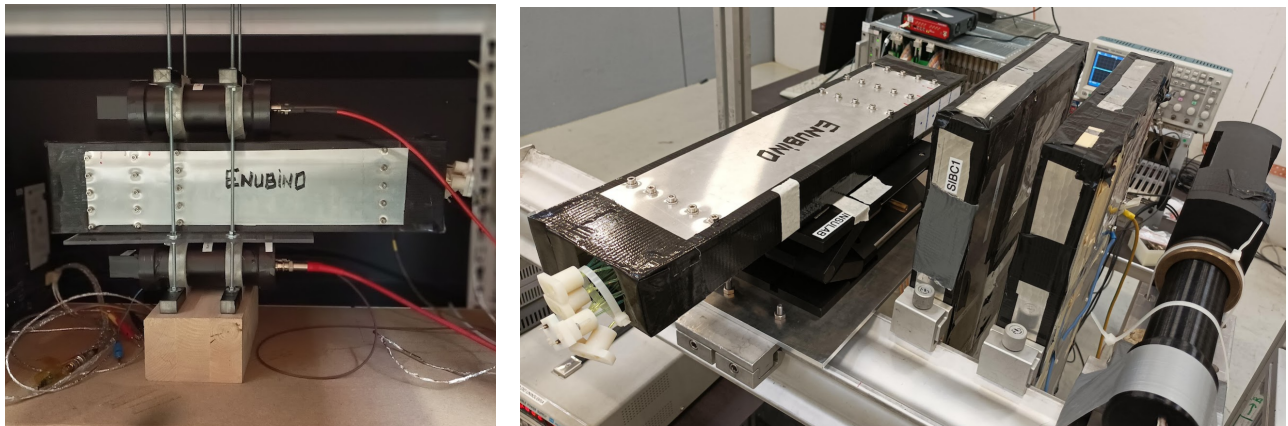


Figure 6: The ENUBINO prototype exposed to cosmic rays and beams at the CERN-PS.

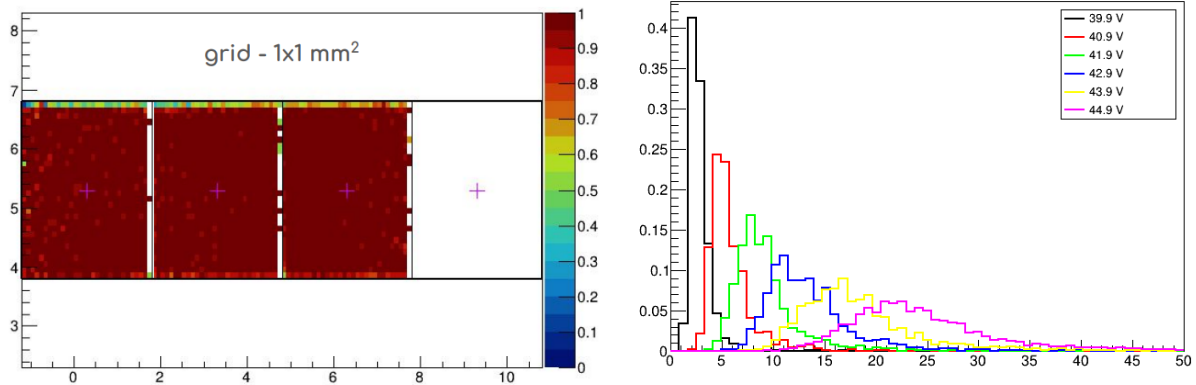


Figure 7: ENUBINO: efficiency maps (left) and m.i.p. signals as a function of the over-voltage of the chosen Hamamatsu SiPMs, in mV (right).

parameters concerning the apertures and shape of the last two collimators (Fig. 8, left). For each configuration the figure of merit (f.o.m.) has been defined as the ratio between the number of background positrons and pions (i.e. not coming from kaon decays) impinging on the tagger and the number of kaons entering the tagger. The scan was run on the CC-IN2P3 cluster using 100 beamlines for each iteration and a total number of about 100 iterations taking from 5 to 8 hours each. This scan has led to a reconfiguration of the beamline, with an improved figure of merit: the previous one was based on a less realistic simulation of the backgrounds (G4beamline). The convergence proved to be effective and achievable in a reasonable amount of time.

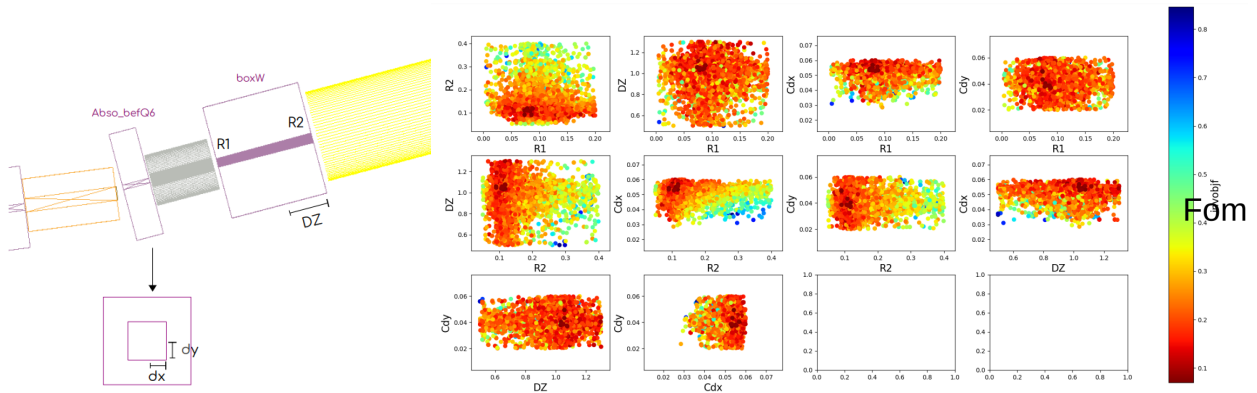


Figure 8: Left: optimization parameters (R_1 , R_2 , dx , dy , Δz). Right: dependence of the f.o.m. on the optimization parameters.

This first exercise allowed us to understand several ways to further improve the results:

- The implemented GEANT4 simulation makes possible to gather the origin information of

every particle (as parent particle, kinematics, specific decay channel of production, beamline element, and so on). This showed that most of the residual positron background was produced in the absorber before the last quadrupole, whose range of variation in the optimization process was not sufficiently wide. By removing it we could improve the positron background by about a factor 6. This monitoring tool hence proved extremely useful to debug the procedure and introduce significant improvements with simple changes.

- Notwithstanding the reduction in the absolute number of background particles the gain in the final purity of reconstructed positrons was not so high since the distributions of background and signal were more similar to each other with respect to previous beamline designs. This has triggered a redefinition of the figure of merit by taking into account also the basic characteristics of the signal and background distributions in energy and position along the tagger.
- In order to use a refined f.o.m. it is very important to reduce the running time and base the selection on a large-enough statistical sample of signal and background events. In this spirit we have conducted studies to understand if it is possible to avoid simulating the full spectrum of particles at the target exit without biasing the backgrounds significantly. We have concluded that, restricting to target particles with momenta between 7 and 100 GeV, we gain about a factor three in CPU time while keeping the background almost unaltered. Furthermore we have verified that with these cuts the original and the new background levels have the same dependency on the variation of parameters, i.e. their ratio remains about constant. This means that the redefined background can be safely used in the genetic algorithm as it would preserve the optimization maxima. Additional tricks to increase statistics are being implemented. First, kaons entering the tagger are treated by an auxiliary simulation that fixes the K_{e3} branching ratio to 100% (roughly a factor 20 gain). In addition we are studying the possibility to fit the spatial and angular distributions of mesons entering the tagger with smooth functions (p, θ, ϕ) and extract events from those probability functions.

In summary this approach seems quite powerful but we have not managed to exploit it fully yet. The present beamline (TLR6v4 in our jargon) has performances not much different than the ones that we already reported in the 2021 report but it is based on a more reliable background simulation without the approximations used previously with G4beamline. Fig. 9 summarizes the state of the art achieved with this version of the beamline in the identification of positrons and muons from kaons, employing the PID algorithms already described in [1]. With the improvements that we have just described we expect an additional increase in the S/N ratio keeping the running time of the experiment in the 2-3 year ballpark.

The current design (TLR6v4) has also been recently ported to FLUKA-CERN. Figure 10, top, shows the FLUKA implementation that includes proper shielding around the magnetic elements. As an example, in the bottom plot of the same figure we show the energy deposition for positive pions which demonstrates also how the magnetic fields and the geometry have been implemented correctly. With respect to the past we have added in the simulation plots on the residual activation in the

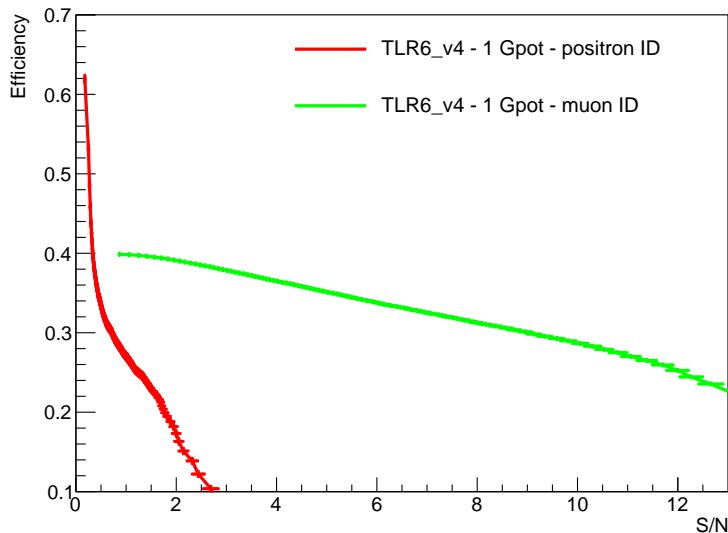


Figure 9: Efficiency in the identification of positrons (in red) and muons (in green) from kaons as a function of the signal-to-noise ratio with the current implementation of the beamline.

materials (Fig. 11) which is a key information to determine the accessibility to the instrumented decay tunnel for possible maintenance or overhauling of the equipment. The FLUKA simulation of TLR6v4 (Fig. 12) also confirms that the neutron yields are compatible with the use of a SiPM readout in a specialized calorimeter with a dedicated borated-PE shielding (see Sec. 1.1).

The work on the multi-momentum beamline is also progressing. The simulation implements a detailed field map both in the core of the magnets and in the iron (Fig. 13). Furthermore it uses models based on real magnets that have been already tested and characterised at CERN. This process is taking a significant effort in terms of CPU and simulation time due to the need of implementing a fine-mesh for the simulation in order to avoid artifacts in the shape of the magnetic field. Besides exploring which is the margin of improvement to get neutrino monitored fluxes a lower energies, it will set a limit on the effect of using a detailed magnetic field map.

1.3 Assessment of systematic uncertainties

The framework for estimating the reduction in the systematic uncertainty on the flux with ENUBET has grown a lot during the last year [3]. The G4beamline and GEANT4 simulation of the beamline are redundant, giving the chance to cross-check the resulting performance. Furthermore, the asset of a GEANT4 implementation is to provided information on particle decays and histories. This is essential for the propagation of the systematics, from their sources up to the neutrino fluxes ([4]).

Hadroproduction data are used as input to reweigh the MC events giving origin to neutrinos.

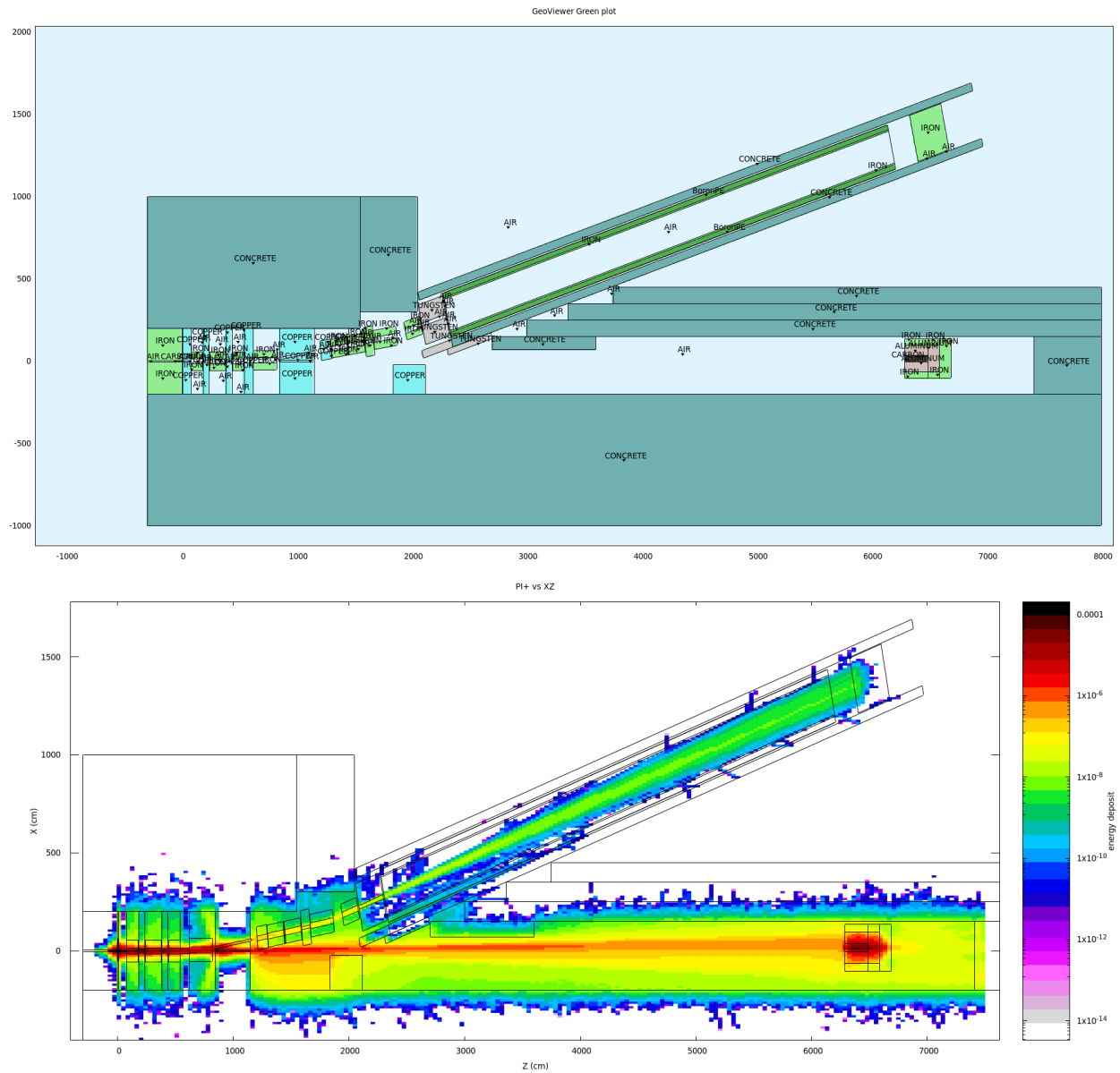


Figure 10: FLUKA simulation of TLR6v4. Geometry and materials (top) and energy deposit from π^+ (bottom).

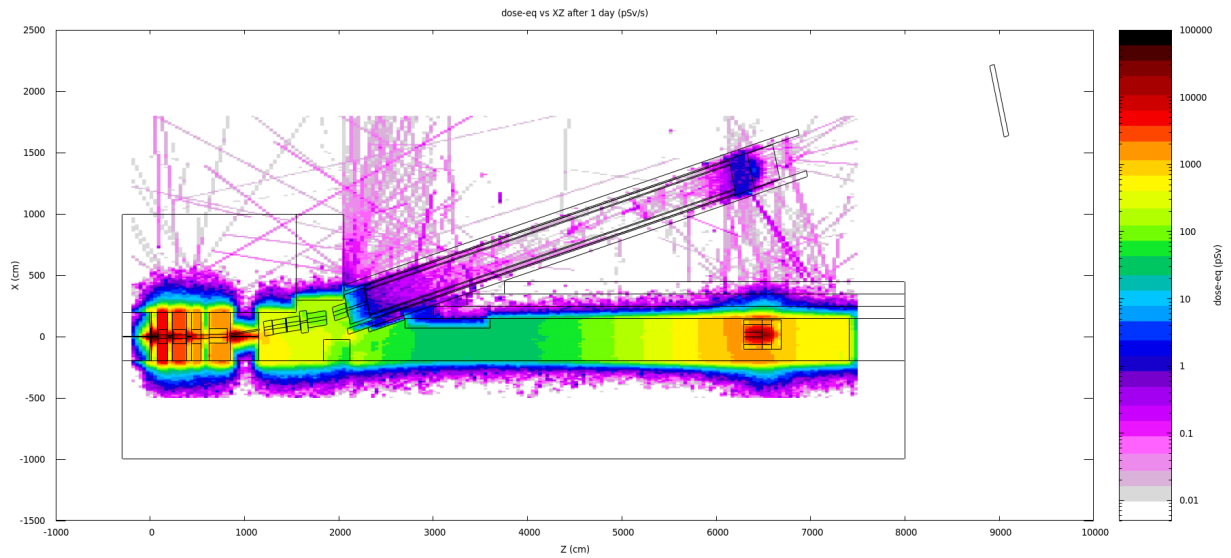


Figure 11: Equivalent dose in pSv/s after 1 day. In the tagger typical values of 0.05 pSv/s are observed (180 pSv/h).

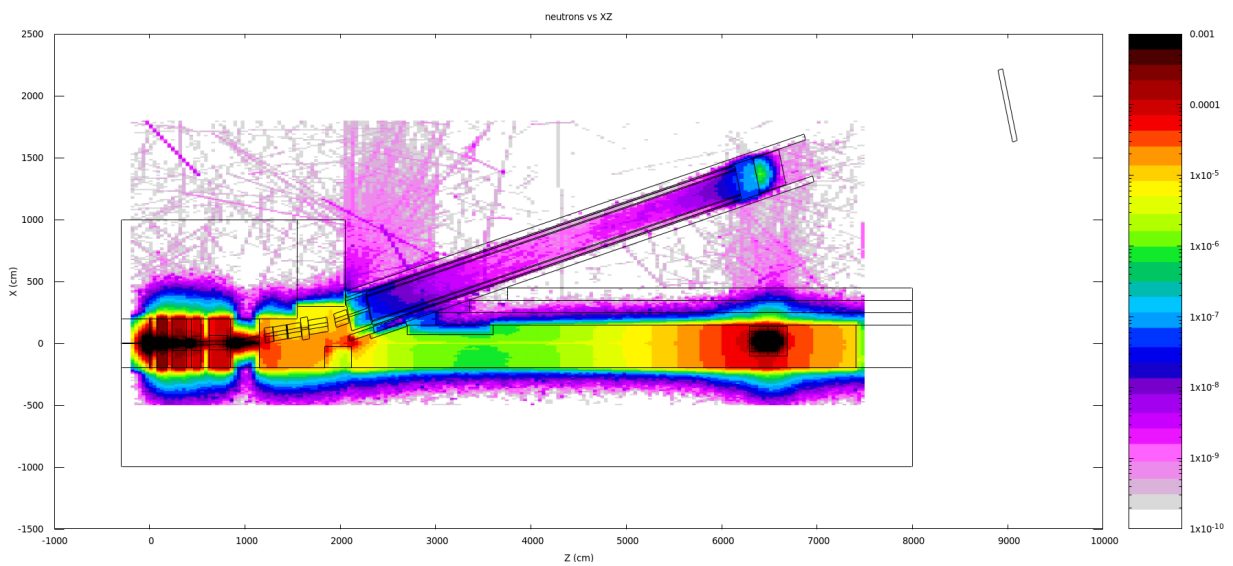


Figure 12: FLUKA simulation of TLR6v4. Neutron fluence.

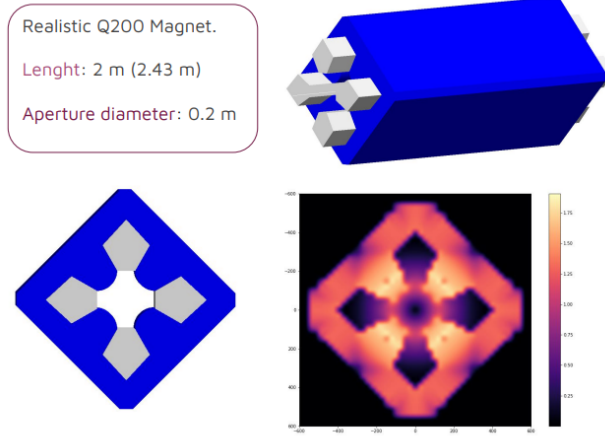


Figure 13: Implementation of magnetic maps for the multi-momentum beamline implementation.

From the reweighed events a nominal neutrino flux at the detector is obtained. The covariance matrix from hadroproduction data is used to extract new values for the hadroproduction parameters, within their uncertainties, and thus get a set of N reweighed MC events. The N realizations of the MC events allow to determine the covariance matrix of the nominal neutrino flux. This covariance matrix encodes the uncertainty on the neutrino flux due to hadroproduction before exploiting the lepton distributions in the tagger. In a similar manner, systematics related to beamline parameters are propagated to the neutrino flux. The simulation with the beamline parameters set to their central values provides the nominal neutrino flux distribution, while the varied realization of the flux is obtained by tweaking the parameters within their uncertainties.

Given the correlation between the lepton observables and the produced neutrinos (monitoring technique) a constraint on the neutrino flux can be set. By means of extraction of different possible values for the parameters affected by the uncertainties, using their covariance matrix, and reweighing the MC events, nominal and $\pm 1\sigma$ distributions for the lepton observables are computed.

A signal plus background model PDF is built from the nominal and the $\pm 1\sigma$ lepton observables (model templates) and the minimization is performed using the ROOFIT package. The variation in the number of observed leptons and in the shape of their distributions, due to hadroproduction and beamline uncertainties, are modeled through corresponding parameters, $\vec{\alpha}$ and $\vec{\beta}$, included in the PDF. An extended maximum likelihood fit approach is adopted, where the parameters $\vec{\alpha}$ and $\vec{\beta}$ are constrained by their pdfs resulted from the uncertainty propagation described above. From the model PDF a set of toy-MC experiments is produced, where each experiment is obtained by extracting the parameters affected by systematics from their covariance matrices. A posteriori values for the parameters are obtained by a fit to each toy-MC: these constrained parameters, with reduced errors, are used to reweigh the MC. In turn, a post-fit reweighed neutrino flux (constrained neutrino flux) and corresponding covariance matrix are computed.

In the previous report we showed that the machinery was working using a toy MC (no bias, assessment of post-fit errors). More recently we managed to demonstrate the reduction of uncertainty introduced by the tagger constraint using the full G4 simulation. The hadroproduction model is a realistic one derived from a fit to real data obtained by the NA56/SPY experiment [5] using 400 GeV proton interactions. In addition both K_{e3} (for ν_e) and $K_{\mu 2}/K_{\mu 3}$ (for ν_μ) data sample constraints have been implemented.

Figure 14 shows preliminary results in which the reduction of the systematics uncertainties after the fit constraint on lepton variables is visible by comparing the uncertainty envelope before and after the fit. We are presently assessing the impact of the facility parameters (magnetic fields, alignments) following a similar procedure.

1.4 Collaboration, synergies with other projects

Other significant new elements that emerged during the last year:

- The ERC programs was further extended up to November 2022 in view of the situation related to the COVID pandemic.
- Participation to the activities of Physics Beyond Colliders. We have been actively participating to the workpackage on conventional neutrino beams with regular presentations on the beamline development with useful interactions with other users (NA62, NUTAG) and CERN experts. Furthermore we are contributing to the workpackage on searches for new physics.
- The nuSTORM/ENUBET workshop in Cagliari. A special joint plenary session with nuSTORM was organised on 9/9/2021 ([6], [7]). It was an important occasion to get a broad visibility and discuss possible scenarios in which both experiments could be fed by mesons produced in a common target station [8]. A scenario involving a siting at the muon colliders test facility at the PS was discussed ([9]).
- We recently submitted the ENUBET physics case to the Snowmass 2021 DPF Community Planning Exercise [10].
- We started a collaboration with the PIMENT project ([11]), funded by the French ANR for the next 3 years with Thomas Papaevangelou from CEA-Saclay as PI. It will deal with the possibility of upgrading the ENUBET t_0 -layer with a detector based on the PICOSEC thin gap Micromegas detector to achieve sub-100 ps time resolutions on large areas.
- Two new PhD students from Thessaloniki University (advisor Prof. S. Tzamarias) will start working in ENUBET on waveform reconstruction and the identification of forward muons from pion decays.

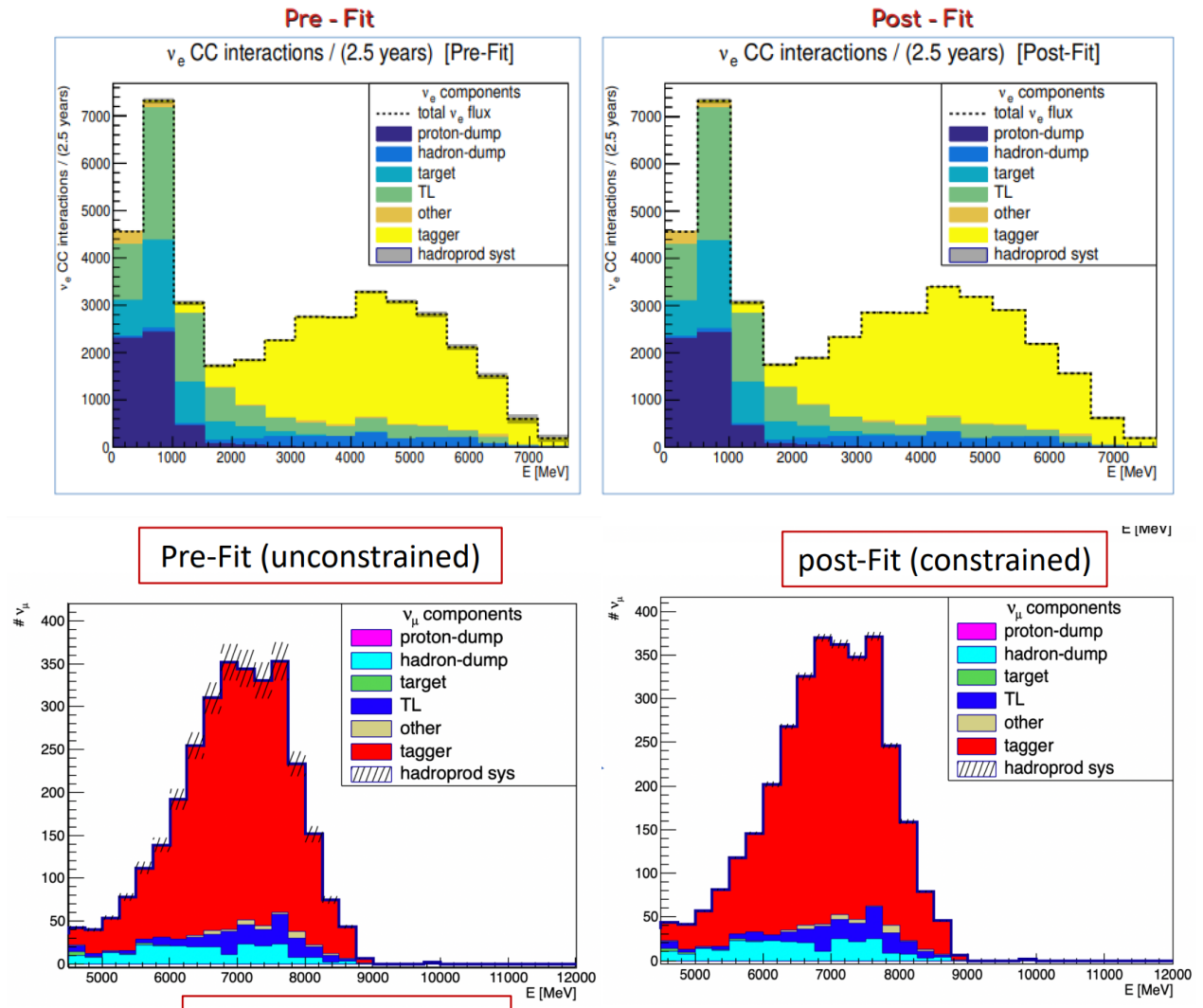


Figure 14: Example of the reduction of hadroproduction uncertainties on ν_e and ν_μ spectra after the constraint given by fitting the lepton spectra reconstructed in the tagger.

References

- [1] NP06/ENUBET Annual Report for the SPSC (2021) <https://cds.cern.ch/record/2759849?ln=en>.
- [2] M. Pari, *Development and optimization of the ENUBET beamline* talk at nuFact2021. <https://indico.cern.ch/event/855372/timetable/#20210909.detailed> PoS(NuFact2021)028 .
- [3] A. Branca, *Fluxes and systematics reduction with decay monitoring* talk at nuFact2021. <https://indico.cern.ch/event/855372/timetable/#20210909.detailed>. PoS(NuFact2021)030.
- [4] M. Kordowsky, *Error bands from the many universes method*, Minerva Document 7433, <https://minerva-docdb.fnal.gov/cgi-bin/ShowDocument?docid=7433>
- [5] The NA56/SPY Collaboration., Ambrosini et al., G. Measurement of charged particle production from 450 GeV/c protons on beryllium. Eur. Phys. J. C 10, 605–627 (1999)
- [6] NuFact 2021: The 22nd International Workshop on Neutrinos from Accelerators. Cagliari (IT), 9/9/21 ENUBET-nuSTORM joint plenary session. <https://indico.cern.ch/event/855372/timetable/#20210909.detailed>
- [7] A. Longhin, *Summary of the nuSTORM/ENUBET workshop* nuFact2021. <https://indico.cern.ch/event/855372/timetable/#20210911.detailed>.
- [8] J. Pasternak, *Design of a common beam line for ENUBET/nuSTORM* nuFact2021. <https://indico.cern.ch/event/855372/timetable/#20210909.detailed>.
- [9] Rui Franqueira Ximenes, *Possible layouts at CERN.* nuFact2021. <https://indico.cern.ch/event/855372/timetable/#20210909.detailed>.
- [10] *Enhanced Neutrino BEams from kaon Tagging (ENUBET)* A. Longhin, F. Terranova (on behalf of the ENUBET Coll.) <https://arxiv.org/abs/2203.08319>.
- [11] PIMENT ANR kickoff meeting, <https://cernbox.cern.ch/index.php/s/22RrbK11KNyYXEQ>.